Hindawi
International Journal of Polymer Science
Volume 2018, Article ID 5049728, 7 pages
https://doi.org/10.1155/2018/5049728

Research Article

Evaluation of the Morphology and Biocompatibility of Natural Silk Fibers/Agar Blend Scaffolds for Tissue Regeneration

Luong Thu-Hien,[1] Nguyen Thanh-Truc,[1] Vo Van Toi,[1] Huynh Chan Khon,[1] Bui Chi Bao,[2] Vo Van Thanh Niem,[2] Mai Ngoc Tuan Anh,[3] Nguyen Dai Hai,[4,5] Pham Dinh Chuong,[6] and Nguyen Thi Hiep[1]

[1] *Tissue Engineering and Regenerative Medicine Group, Department of Biomedical Engineering, International University, Vietnam National University, Ho Chi Minh City (VNU-HCMC), Ho Chi Minh City 700000, Vietnam*
[2] *The Center for Molecular Biomedicine, University of Medicine and Pharmacy, Ho Chi Minh City 700000, Vietnam*
[3] *Research Laboratories of Saigon Hi-Tech Park, Ho Chi Minh City 700000, Vietnam*
[4] *Institute of Applied Materials Science, Vietnam Academy of Science and Technology, 01 Mac Dinh Chi, District 1, Ho Chi Minh City, Vietnam*
[5] *Graduate University of Science and Technology, Vietnam Academy of Science and Technology, Hanoi, Vietnam*
[6] *Faculty of Applied Sciences, Ton Duc Thang University, Ho Chi Minh City 700000, Vietnam*

Correspondence should be addressed to Nguyen Thi Hiep; nthiep1981@gmail.com

Received 26 August 2017; Accepted 20 November 2017; Published 18 January 2018

Academic Editor: Kajal Ghosal

This study was aimed to develop a tissue engineering scaffold by incorporation of *Bombyx mori* silk fiber (BMSF) and agar. This promised the improvement in enhancing their advantageous properties as well as limiting their defects without occurring chemical reactions or crosslink formation. The morphology and chemical structure of scaffolds were observed using scanning electron microscope (SEM) observation and Fourier transform infrared (FT-IR) spectra. The SEM results show that scaffolds containing BMSF have microporous structures, which are suitable for cell adhesion. Agar scaffolds, by contrast, had much more flat morphology. FT-IR spectra confirm that no modifications to BMSF happened in scaffolds, which indicates that there was no chemical reaction or crosslink formation between silk and agar in this process. Furthermore, the biocompatibility of scaffolds was performed in the mouse's subcutaneous part of the dorsal region for 15 days, followed by Haematoxylin and Eosin (H&E) staining. H&E staining results demonstrate that scaffolds had good biocompatibility and there was no sign of the body rejection in all of samples. The results from animal study show that SA scaffolds have the most stable structure for cell adhesion compared with those single materials.

1. Introduction

Silk proteins are generally defined as protein polymer extracted from silkworm's cocoons. In its natural form, silk is composed of fibroin as an inner layer and a sericin coating as an outer layer [1]. Silk fibroin protein can be used as a potential biomaterial in biomedical applications due to its unique mechanical and biochemical properties, such as high tensile strength, good degree of toughness and elasticity, high permeability to oxygen and water, relatively low thrombogenicity, morphologic flexibility, and the support for cell adhesion and growth [2–4]. In contrast, there are several reports concerning immune responses which relate to macrophage activation, in vivo inflammation or skin irritation, and skin allergies of sericin proteins [2, 5]. This is the reason why, for biomedical and clinical application, sericin protein should be eliminated completely from the silk fibers via degumming process before any further application [3, 4].

Thanks to outstanding biophysical properties such as high tensile strength, high elasticity, and low biodegradation rate, BMSF becomes a promising candidate for tissue engineering application with high mechanical durability such as ligament, bone, tendons, or muscle. Moreover, BMSF has also comparatively low biodegradation rate, which is suitable to

prolong the healing process of the tissues or organs that need a long time to regenerate such as bone. Compared with regenerated silk fibroins, which require to be dissolved into silk solution and restructured secondary structure, BMSF producing process is more simple and economically efficient [6]. Moreover, in other researches, BMSF scaffolds were investigated for ligament and vascular graft application using the physical fabrication method (Knitting) [7–9]. However, the knitting method is mainly for creating flat mesh and is not available for more complicated structure such as 3D scaffold. Therefore, in this study, another natural polymer was investigated as the adhesive factor blending in the BMSF structure in order to increase the stability of the BMSF scaffold. Agar is a popular biological polymer that is used in tissue engineering due to its consistency, controllable size, elasticity, and adjustable concentration-dependent mechanical characteristics [10]. Agar has the favorable biocompatibility, moderate intention strength, and low degradation rate [11, 12].

The aim of our study is to compare the complex of two natural polymers, BMSF and agar, with each single one to figure out the advantage of combination base on their porous structure and biocompatibility for tissue regeneration. The morphology and chemical properties of scaffolds were observed and analyzed using SEM observation and FT-IR spectra. To evaluate biocompatibility of scaffolds, mice model was used in this study.

2. Materials and Methods

2.1. Materials. *Bombyx mori* silkworm cocoons were supplied by Viet Silk Limited Co., Lam Dong, Vietnam. The supplied cocoons were in fresh status and did not undergo any thermal, mechanical, or chemical treatment. Sodium hydroxide (NaOH), sodium carbonate (Na_2CO_3), citric acid ($C_6H_8O_7$), and ethanol (C_2H_5OH) were purchased from Xilong Chemical, Ltd., China. Agar strips were supplied by Hoang Yen Co., Ltd., Vietnam. The animal study was performed on Swiss Albino mice, about 30 g, provided by Pasteur Institute, Ho Chi Minh City, Vietnam. Hematoxylin and Eosin (H&E) staining chemicals, including Haematoxylin, Eosin, and Xylene, were purchased from Sigma-Aldrich, Inc., Germany.

2.2. Degumming Process. SF was prepared by elimination of sericin protein from raw cocoons via degumming process. In short, degumming solution was made by adding natural soap to 0.06 M Na_2CO_3 solution to adjust its pH to 11.6. Cocoons after removing silkworm were treated with degumming solution two times: 30 minutes at 95°C and 15 minutes at 80°C, respectively. Then the degummed silk fibers were rinsed thoroughly with warm water to remove all of sericin gel-like coat before drying at 40°C. The product of this process was long and bright white silk fibers.

2.3. Scaffolds Preparation. For the agar scaffolds (called A), 0.02% agar was soaked in distilled water for 30 minutes at room temperature and then boiled to 80°C with stirring for 2 hours until it completely turned into a transparent homogeneous solution. The agar solution was poured into a mold and cooled to room temperature.

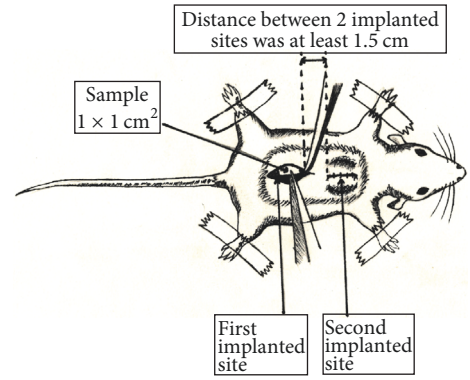

Figure 1: Cartoon depicting surgical model for subcutaneous implant study.

For the agar and SF complex scaffolds (called SA), SF was first placed into the square mold and then warm agar solution was poured to fill the mold (SF : agar solution = 1 : 20 w/w). The silk-agar mold was cooled to room temperature.

For the SF scaffolds (S), the moist silk fibers were fixed under high pressure at 45°C for 24 hours to evaporate all the humidity and then cooled to room temperature.

All three samples were cut to the shape of $10 \times 10 \times 1\,mm^3$ for in vivo and $20 \times 40 \times 1\,mm^3$ for other tests. The cut samples were freeze-dried (ILSHIN Freeze Dryer, FD Series, USA) to eliminate all of the water contained.

2.4. Scanning Electron Microscopy (SEM). The surface morphology and pore geometries of three sample groups (S, A, and SA) were observed using SEM (HITACHI scanning electron microscope, S-3000H, Japan) under vacuum and recorded digitally.

2.5. FT-IR Analysis. The components of scaffolds were characterized with FT-IR in the frequency range of 400–4000 cm^{-1} (TENSOR II FT-IR spectrometer, Bruker, Germany).

2.6. Animal Study. In order to evaluate the biocompatibility of three sample groups, prepared scaffolds ($10 \times 10 \times 1\,mm^3$) were sterilized by UV light (20 minutes) before being subcutaneously implanted at dorsal region under general anesthesia and antiseptic conditions (Figure 1). The operation process was performed following the policy of Institutional Animal Care and Use Committee of International University, Vietnam National University, Ho Chi Minh City, Vietnam [13]. In detail, mice were anesthetized with dimethyl ether, their hair was shaved at their back, and they were fixed on a table. The implanted site was cleaned by povidone solution and PBS buffer before making the laceration for inserting the samples [14]. The experimental study involved 9 female Swiss Albino mice (3 mice for each group). After 15 days, mice were sacrificed, and then the regenerated area with the scaffold was extracted. The extracted sample was fixed by 3% formaldehyde and then sectioned using a cryomicrotome before staining by Hematoxylin and Eosin (H&E) stain. H&E

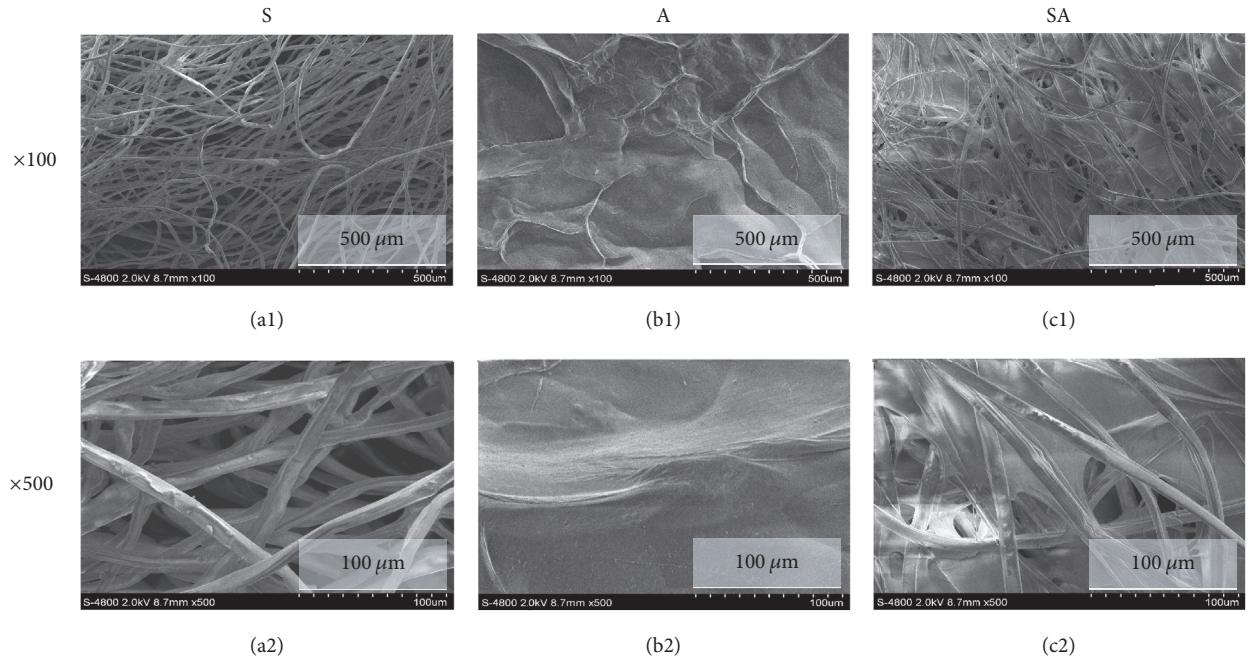

FIGURE 2: SEM images of 3 studied scaffolds at 2 magnifications (×100 and ×500): (a1, a2) S scaffold, (b1, b2) A scaffold, and (c1, c2) SA scaffold.

stained samples were observed by light microscope (Nikon Eclipse, Ti-U Series, Japan).

3. Results

3.1. Scanning Electron Microscope (SEM). The SEM was performed to evaluate the morphology of each scaffold. The BMSF in Figures 2(a1) and 2(a2) have no hierarchical order and are flexible when mechanically deformed in a variety of directions; however, the surface area for cell adhesion is limited to the surface area of the fibers in the matrix, which motivates inclusion of a hydrogel between the fibers to increase the numbers of cells adhering to the matrix. The separation of each SF observed in Figures 2(a1) and 2(a2) represents the lack of coherence in S scaffold, leading to the loosening of scaffold's shape in humid condition, which could affect cell adhesion and lost cell-anchorage role and reduce ECM generation rate in vivo. Therefore, agar was introduced to increase the stability of the structure of the silk scaffold. Figures 2(b1) and 2(b2) show the SEM images of A scaffold with no pore observed on the surface, which inhibited cell attachment. Figures 2(c1) and 2(c2) of SA scaffold show the combination of the best features of S and A samples: stability and high porosity. The pore system of SA scaffold provided a good condition for cell attachment, proliferation, and migration as well as vascularization. The variability of diameters of pores is due to the randomness of the silk fibers.

3.2. FT-IR Analysis. To examine the chemical interaction between silk and agar in the SA sample, the FT-IR spectra of S, A, and SA samples in the frequency range of 400–4000 cm^{-1} were depicted (Figure 3). The spectrum of S scaffolds shows the strong absorption peaks around 1622 cm^{-1} (amide I),

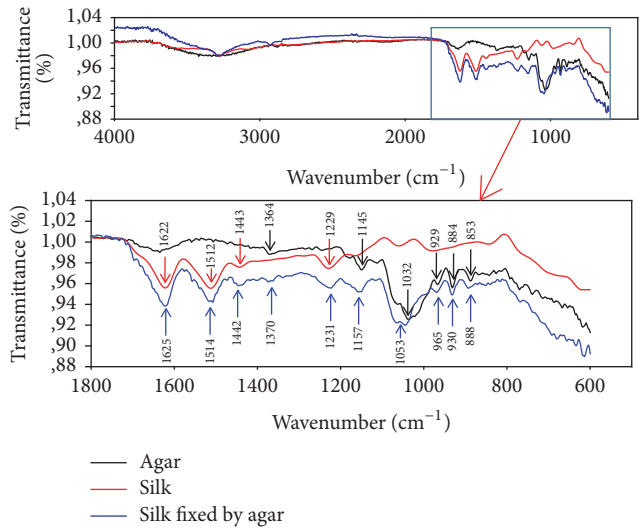

FIGURE 3: FT-IR spectra of 3 scaffolds: (a) in frequency range of 400–4000 cm^{-1} and open box; (b) in frequency range of 600–1800 cm^{-1}. Red, black, and blue arrows showed main peaks of S, A, and SA scaffolds, respectively.

1512 cm^{-1} (amide II), and 1229 cm^{-1} (amide III) corresponding to characteristic protein structure [15, 16]. In A scaffold, a polysaccharide structure, the most intense band observed at 1032 cm^{-1} is common to all the polysaccharide molecules and had contributions from several vibration modes, such as C–O, C–O–H, and C–C stretching [17]. The strong band at 929 cm^{-1} assigned to the presence of 3,6-anhydrogalactose residue was common to agar [18]. The feature bands of agars and silk protein are all observed in SA spectra. The peaks' positions of SA scaffold were just slightly changed from the

main peaks of S and A's spectroscopy (1625 cm^{-1} for amide I, 1514 cm^{-1} for amide II, 1231 cm^{-1} for amide III, and 1053 and 930 cm^{-1} for polysaccharide molecules). There was no strange peak which proved that the addition of agar in SA blends did not cause structural conformation modifications to silk fibroin fibers.

3.3. Animal Study. In order to test biocompatibility, the scaffolds were analyzed by subcutaneous implantation in mice. Figure 4 shows the photographs of postimplantation of A, S, and SA scaffolds after 5 minutes, 2 days, 10 days, and 15 days. Figure 4(a) showed that the S scaffold got severely deformed compared with the origin fixed shape, which was 10 $\times 10 \times 1\,mm^3$. This deformation occurred right after putting in the moist condition of the body. However, A and SA scaffolds still kept their shape during implantation process (Figures 4(b) and 4(c)). After 2 days, the implanted site's wounds were all closed with no unusually colored area.

Figure 5 shows the H&E staining of the scaffold after 15 days at 2 magnifications: ×200 and ×600. Figures 5(a), 5(b), 5(e), and 5(f) show that the cells were getting started to attach into the silk-contained scaffolds (S and SA) with high density. In another case, in Figures 5(c) and 5(d) of A scaffold, there is no sign of cell adhesion on agar fiber or surrounding area. Compared to A scaffold, the highly porous structure of S and SA scaffolds mimicked natural ECM structure and significant increase of cell attachment.

The animal test results indicate that the combination of silk fibers and agar created the scaffolds which could strongly support cell adhesion and proliferation with their high porosity, cohesion, and structure durability.

4. Discussion

4.1. Scanning Electron Microscope (SEM). Degumming is a thermochemical treatment applied on silkworm cocoons to eliminate glue-like coating sericin, remove other impurities, and extract BMSF. In sericin, about 80% amino acid has hydrophilic lateral group. Sericins that coat silk fibroin fibers react with each other by numerous noncovalent intermolecular interactions, such as hydrobonds. To weaken these interactions, medium bases as Na_2CO_3 are used under thermal condition. According to SEM results, there were no sericin as well as other impurities and the fact that there is no sign of destruction or damage on the surface of silk fibers implies that the degumming process was appropriative [4].

The discrete arrangement of SF observed in Figures 2(a1) and 2(a2) represents the lack of stability and coherence in S sample, which could affect cell adhesion in vivo task. On the other hand, agar was introduced as the factor to enhance the stability and withstand deformation loading, either static or dynamic, during cell proliferation [19]. The combination of silk and agar in SA sample increased the cohesion and unity of the scaffold and provided the pore system for cell attachment and cell migration of most mammalian anchorage-dependent cell types [20]. Moreover, the porosity of silk scaffold is the advantage for capillaries growth. The noncompact structure also influences the degradation behavior because the distribution of pores is a good condition for cell migration, cell proliferation, tissue formation, enzymes binding, and hydrolysis behavior displaying [21–24].

4.2. FT-IR Spectra. As Figure 3 shows, SA scaffold's main peaks are combination of silk and agar's peaks, and there was no strange peak appearance in SA spectroscopy. The result indicates that there was no chemical reaction or crosslink formation between silk and agar. Silk and agar are well investigated in other studies [9, 10, 25] and were proven to have good biocompatibility and no toxicity toward the body system. This result confirms that there is no change of properties of initial components. In other words, the SA group inherited all the good characteristics of both silk protein and agar.

4.3. Animal Study. The previous studies show that agar has good biocompatibility and can be considered as a potential adhesive factor for biomaterial structure but it does not provide sufficient support for cell adhesion [26, 27], while BMSF has the vigorous ability to support cell attachment and growth but it is hard to keep the fiber mesh in the humid condition [28, 29]. So we attempt to combine two ingredients, agar and BMSF, to improve shortcomings of those biomaterials. The cell's viability, adhesion, and proliferation on the scaffold are used to indicate the biocompatibility and appropriateness of medical application. Because proliferation of most mammalian cell types depends on anchorage, the implanted scaffold must provide a suitable ability for cell adhesion, proliferation, and migration [28, 29]. In this study, S and SA performed as a great potential biomaterial for mammalian cell migration, cell attachment, and long-term viability supporting, while A scaffold was not due to its structure and properties.

In vivo results indicate that S scaffold performed as a potential biomaterial for cell adhesion but it lacked the ability to maintain its shape; on the contrary, A scaffold preserved the shape well but has no cell adhesion feature. The combination of agar and BMSF provided the ability to utilize the good characteristics of those two components. Moreover, this combination enhanced the cell adhesion and ECM regeneration.

5. Conclusion

Addition of agar to support the stability of BMSF structure was not only increasing the porosity, interconnected pore, and cohesion of silk fibers but also mimicking ECM porous structure and strongly supported cell attachment in vivo. The SEM observations indicate that SA scaffold has a porous structure, which is suitable for cell culture. The animal study shows that both S and SA had good biocompatibility, cell adhesion supporting, viability, and proliferation and promoted ECM generating, while A scaffold was only biocompatible but not supportive for cell attachment or ECM formation. Compared to S scaffold, SA scaffold has great porosity and higher cohesion and structural durability. Further studies, in progress, are necessary to quantify more the physical, chemical, and bioangiogenic bioactivity of SA scaffold.

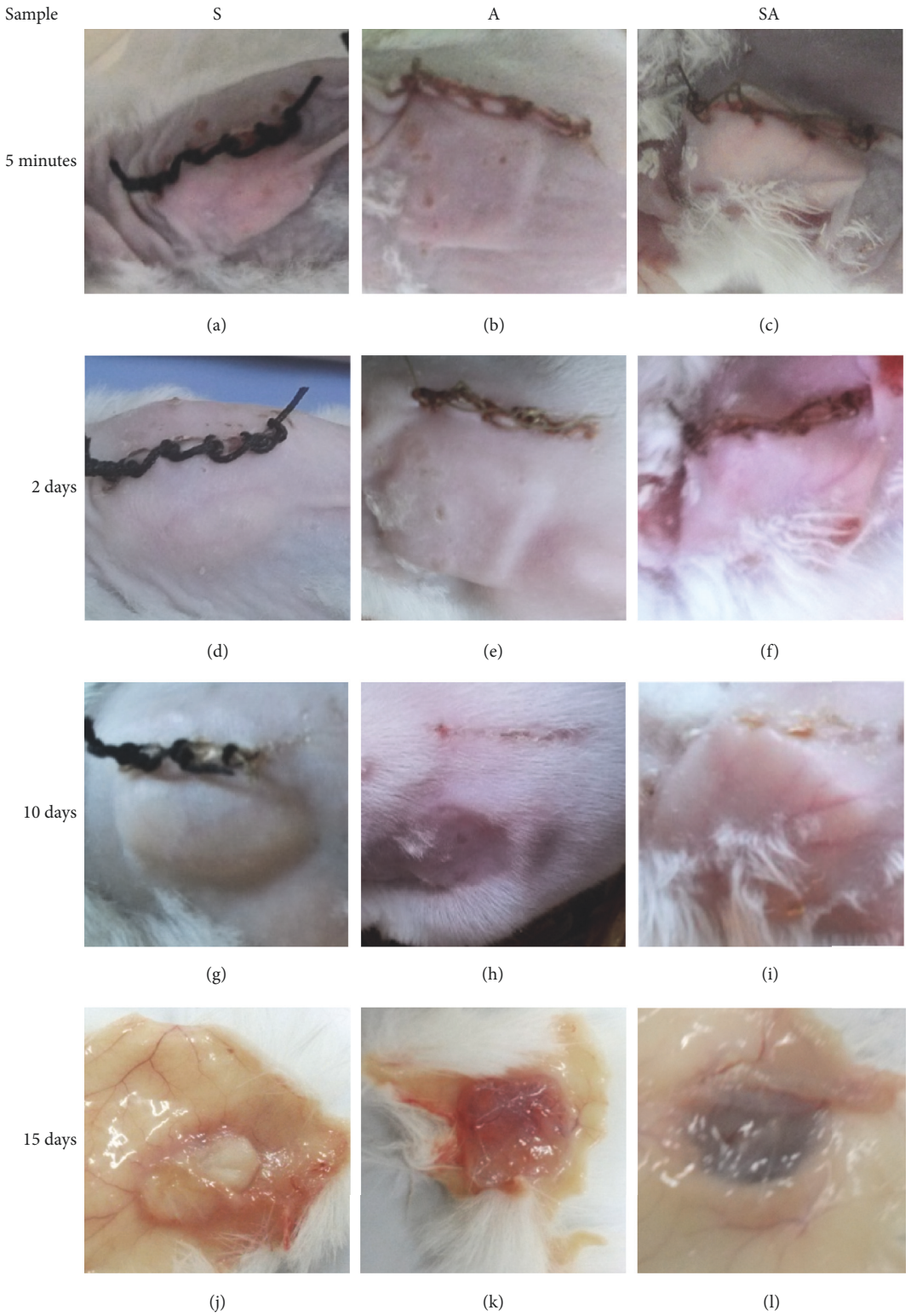

Figure 4: Subcutaneous implantation of 3 samples: (a–c) 5 minutes after implantation of S, A, and SA scaffolds, respectively; (d–f) 2 days after implantation of S, A, and SA scaffolds, respectively; (g–i) 10 days after implantation of S, A, and SA scaffolds, respectively; (j–l) extracted sample of S, A, and SA scaffolds, respectively, 15 days after implantation.

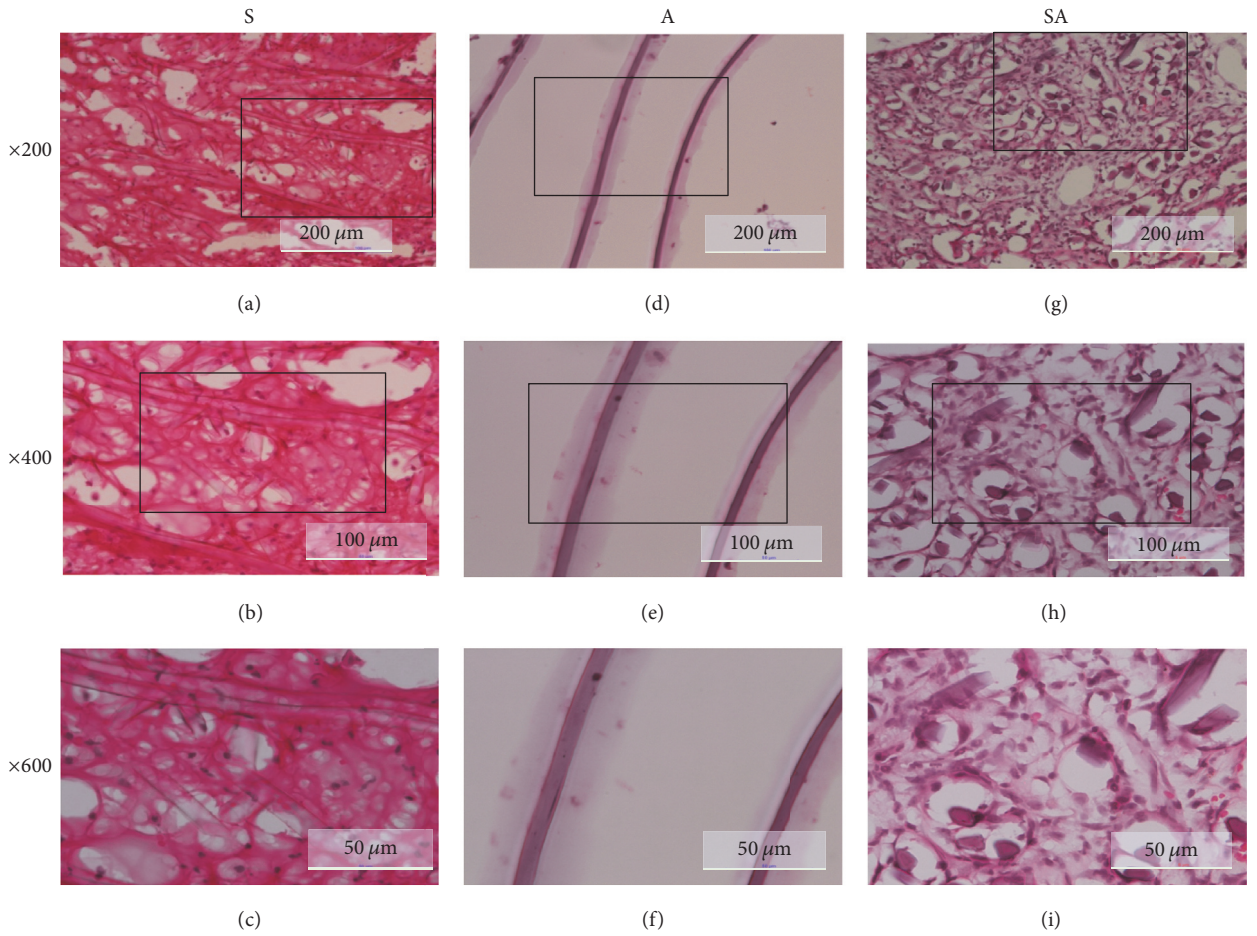

Figure 5: H&E staining of implanted sample after 15 days: (a, b, c) S scaffold, (d, e, f) A scaffold, and (g, h, i) SA scaffold, at 3 magnifications: ×200, ×400, and ×600.

Disclosure

An earlier version of this work was presented as an abstract at ICAS-1 2016: the 1st International Conference on Applied Sciences.

Conflicts of Interest

The authors declare that there are no conflicts of interest regarding the publication of this paper.

Acknowledgments

This research was supported by Vietnam National University, Ho Chi Minh City, under Grant no. 1161/QĐ-ĐHQG-KHCN.

References

[1] V. Kearns, A. C. Macintosh, A. Crawford, and P. V. Hatton, *Silk-Based Biomaterials for Tissue Engineering*, R. R. N. Ashammakhi and F. Chiellini, Eds., 2008.

[2] S. Fan, Y. Zhang, H. Shao, and X. Hu, "Electrospun regenerated silk fibroin mats with enhanced mechanical properties," *International Journal of Biological Macromolecules*, vol. 56, pp. 83–88, 2013.

[3] H. Fan, H. Liu, S. L. Toh, and J. C. H. Goh, "Anterior cruciate ligament regeneration using mesenchymal stem cells and silk scaffold in large animal model," *Biomaterials*, vol. 30, no. 28, pp. 4967–4977, 2009.

[4] H. T. Nguyen, H. T. Luong, H. D. Nguyen, H. A. Tran, K. C. Huynh, and T. V. Vo, "Investigate the Effect of Thawing Process on the Self-Assembly of Silk Protein for Tissue Applications," *BioMed Research International*, vol. 2017, Article ID 4263762, 2017.

[5] D. N. Rockwood, R. C. Preda, T. Yücel, X. Wang, M. L. Lovett, and D. L. Kaplan, "Materials fabrication from Bombyx mori silk fibroin," *Nature Protocols*, vol. 6, no. 10, pp. 1612–1631, 2011.

[6] S. Liu, C. Dong, G. Lu et al., "Bilayered vascular grafts based on silk proteins," *Acta Biomaterialia*, vol. 9, no. 11, pp. 8991–9003, 2013.

[7] X. Chen, Y.-Y. Qi, L.-L. Wang et al., "Ligament regeneration using a knitted silk scaffold combined with collagen matrix," *Biomaterials*, vol. 29, no. 27, pp. 3683–3692, 2008.

[8] V. T. Nayar, J. D. Weiland, C. S. Nelson, and A. M. Hodge, "Elastic and viscoelastic characterization of agar," *Journal of the Mechanical Behavior of Biomedical Materials*, vol. 7, pp. 60–68, 2012.

[9] Y. Freile-Pelegrín, T. Madera-Santana, D. Robledo, L. Veleva, P. Quintana, and J. A. Azamar, "Degradation of agar films in a humid tropical climate: Thermal, mechanical, morphological

and structural changes," *Polymer Degradation and Stability*, vol. 92, no. 2, pp. 244–252, 2007.

[10] Y. Wu, F. Geng, P. R. Chang, J. Yu, and X. Ma, "Effect of agar on the microstructure and performance of potato starch film," *Carbohydrate Polymers*, vol. 76, no. 2, pp. 299–304, 2009.

[11] S. Ling, Z. Qi, D. P. Knight, Z. Shao, and X. Chen, "Synchrotron FTIR microspectroscopy of single natural silk fibers," *Biomacromolecules*, vol. 12, no. 9, pp. 3344–3349, 2011.

[12] A. Barth, "Infrared spectroscopy of proteins," *Biochimica et Biophysica Acta (BBA) - Bioenergetics*, vol. 1767, no. 9, pp. 1073–1101, 2007.

[13] D. H. Phuc, N. T. Hiep, D. N. P. Chau et al., "Fabrication of hyaluronan-poly(vinylphosphonic acid)-chitosan hydrogel for wound healing application," *International Journal of Polymer Science*, vol. 2016, Article ID 6723716, 9 pages, 2016.

[14] T. T. Nhi, H. C. Khon, N. T. T. Hoai et al., "Fabrication of electrospun polycaprolactone coated withchitosan-silver nanoparticles membranes for wound dressing applications," *Journal of Materials Science: Materials in Medicine*, vol. 27, no. 10, article no. 156, 2016.

[15] M. Sekkal, J.-P. Huvenne, P. Legrand et al., "Direct structural identification of polysaccharides from red algae by FTIR microspectrometry I: localization of agar in Gracilaria verrucosa sections," *Microchimica Acta*, vol. 112, no. 1-4, pp. 1–10, 1993.

[16] E. Gómez-Ordóñez and P. Rupérez, "FTIR-ATR spectroscopy as a tool for polysaccharide identification in edible brown and red seaweeds," *Food Hydrocolloids*, vol. 25, no. 6, pp. 1514–1520, 2011.

[17] S. Bhat, A. Tripathi, and A. Kumar, "Supermacroprous chitosan-agarose-gelatin cryogels: in vitro characterization and in vivo assessment for cartilage tissue engineering," *Journal of the Royal Society Interface*, vol. 8, no. 57, pp. 540–554, 2011.

[18] A. Prokop and M. Z. Rosenberg, "Bioreactor for mamalian cell culture," *Adv Biochem Eng Biotechnol*, vol. 39, pp. 29–71, 1989.

[19] Y. Cao and B. Wang, "Biodegradation of silk biomaterials," *International Journal of Molecular Sciences*, vol. 10, no. 4, pp. 1514–1524, 2009.

[20] Y. Wang, D. D. Rudym, A. Walsh et al., "*In vivo* degradation of three-dimensional silk fibroin scaffolds," *Biomaterials*, vol. 29, no. 24, pp. 3415–3428, 2008.

[21] J. G. Hardy and T. R. Scheibel, "Composite materials based on silk proteins," *Progress in Polymer Science*, vol. 35, no. 9, pp. 1093–1115, 2010.

[22] T.-H. Nguyen and B.-T. Lee, "In vitro and in vivo studies of rhBMP2-coated PS/PCL fibrous scaffolds for bone regeneration," *Journal of Biomedical Materials Research Part A*, vol. 101, no. 3, pp. 797–808, 2013.

[23] A. Sadiasa, T. H. Nguyen, and B. T. Lee, "In vitro and in vivo evaluation of porous PCL-PLLA 3D polymer scaffolds fabricated via salt leaching method for bone tissue engineering applications," *Journal of Biomaterials Science, Polymer Edition*, vol. 25, no. 2, pp. 150–167, 2014.

[24] T.-H. Nguyen, T. Q. Bao, I. Park, and B.-T. Lee, "A novel fibrous scaffold composed of electrospun porous poly(ε-caprolactone) fibers for bone tissue engineering," *Journal of Biomaterials Applications*, vol. 28, no. 4, pp. 514–528, 2013.

[25] A. U. Ude et al., "Bombyx mori silk fibre and its composite: a review of contemporary developments," *Materials & Design*, vol. 57, no. 0, pp. 298–305, 2014.

[26] N. Minoura, M. Tsukada, and M. Nagura, "Physico-chemical properties of silk fibroin membrane as a biomaterial," *Biomaterials*, vol. 11, no. 6, pp. 430–434, 1990.

[27] B. Kundu, N. E. Kurland, S. Bano et al., "Silk proteins for biomedical applications: bioengineering perspectives," *Progress in Polymer Science*, vol. 39, no. 2, pp. 251–267, 2014.

[28] R. M. Prokop A, "Bioreactor for mammalian cell culture," *Adv Biochem Eng Biotechnol*, vol. 39, pp. 29–71, 1989.

[29] W. DF, "Biomaterials and biocompatibility," *Med Prog Technol*, vol. 4, pp. 31–42, 1976.